Lawrence Berkeley National Laboratory

Title
In situ optimization of co-implantation and substrate temperature conditions for Nitrogen-Vacancy center formation in single crystal diamonds

Permalink

Author
Schwartz, J.

Publication Date

DOI

Peer reviewed

In situ optimization of co-implantation and substrate temperature conditions for Nitrogen-Vacancy center formation in single crystal diamonds

J. Schwartz, P. Michaelides, C. D. Weis, and T. Schenkel[1]
Ion Beam Technology Group, Accelerator and Fusion Research Division,
Lawrence Berkeley National Laboratory, Berkeley CA 94720, USA

Abstract

We present first results from *in situ* characterization of Nitrogen-Vacancy (NV) center formation in single crystal diamonds following implantation of low energy nitrogen ions (7.7 keV), co-implantation of hydrogen, helium and carbon ions and *in situ* annealing. Diamond samples were implanted at room temperature or at a temperature of 780º C. We find that dynamic annealing during co-implantation enhances NV-center formation by up to 25%.

1. Introduction

Spins of color centers in diamond, in particular the negatively charged nitrogen vacancy center (NV⁻) are promising quantum bit candidates and they can enable advanced sensing techniques [1-3]. Reliable formation of NV-centers [4-6], their placement with high spatial resolution [4, 5, 7] and the engineering of spin environments for optimal coherence times and spectral stability are formidable challenges [8-10]. Implantation of nitrogen ions into single crystal diamonds with low nitrogen background followed by annealing to >600º C is a simple technique for formation of some NV⁻ centers [4, 5, 11]. NV-centers form during annealing when nitrogen atoms incorporate onto substitutional sites in the diamond crystal lattice [12] and vacancies bind to substitutional nitrogen atoms. The charge states of the NV-center (NV⁺, NV⁰, NV⁻) are determined by the local band structure and can be strongly affected e. g. by a bath of surrounding substitutional nitrogen atoms (P1 centers), other impurities and by surface effects [8, 9, 16]. Reported formation efficiencies, i. e. the number of NV-centers formed per implanted nitrogen atom are currently well below unity [5-7] for low energy implantations (<30 keV) where range straggling is small enough to enable high placement accuracy [4, 5, 7]. Adding vacancies by co-implantation of ion species other then nitrogen can enable their capture into stable NV-centers and has been shown to enhance NV-formation efficiencies [4, 6, 14]. Addition of vacancies is limited by damage accumulation which degrades the crystal lattice irrevocably above a damage threshold of about 10^{22} vacancies/cm³. Annealing of diamonds with damage levels above this threshold leads to irrevocable graphitization, while annealing at damage levels below the threshold re-crystallizes the diamond lattice [15]. Dynamic annealing, i. e. annealing during co-implantation where samples are heated to temperatures above about 600° C [15], can increase conversion of substitutional nitrogen with vacancies into stable NV-centers if processing conditions for favorable kinematics of vacancy generation, dynamic damage repair and low loss rates for already formed NV-centers can be identified. We have configured an *in situ* processing and characterization chamber that enables systematic studies of ion implantation and dynamic annealing conditions for enhanced NV-center formation efficiencies.

---

[1] Corresponding author email: T_Schenkel@LBL.gov

2. Experimental Setup

Figure 1 shows a schematic of our experimental setup. Ion beams enter a vacuum chamber with base pressure of 10^{-7} Torr after mass selection in an ExB filter. Beam intensities were <10 nA/cm^2 and typical dose rates were ~3×10^9 ion/cm^2/s which is low enough to avoid dose rate effects and beam induced heating. The beam energy was set to 7.7 keV for all ion species used in this study and we used a ^{14}N$^+$ ion fluence of 10^{13} cm^{-2} throughout. Co-implantations were performed with hydrogen, helium and carbon ions. The ranges of these ions in diamond as calculated with SRIM [17] are 60 nm (H), 40 nm (He), 13 nm (C) and 11.5 nm (N). All implantations were performed at normal incidence. SRIM does not track the crystal structure of samples and channeling effects for the implants at normal incidence will broaden the range profiles for H and He co-implants, but only minimally for C and N implants at 7.7 keV [7]. Diamond samples were mounted on a goniometer with heatable sample holder with a temperature range up to 1000ºC. We selected an annealing temperature of 780° C in this study. Vacancies become mobile and damage recovery during annealing is effective for temperatures above about 600° C [12, 15], while temperatures above 950° C can lead to surface graphitization. In some ambients, diamond surfaces can also etch during annealing. We did not observe reduced photoluminescence intensities or other evidence for surface etching of diamond samples during extended annealing at 780° C for up to 2 h in vacuum. Following implantation and annealing, NV-centers are excited with a fiber coupled laser (532 nm, 300 mW) and photoluminescence (PL) spectra are collected in a fiber coupled spectrometer. Samples used were electronic grade single crystal CVD diamonds (100) with a nitrogen background <5 ppb from Element 6.

Figure 2 a) shows a series of spectra from a diamond sample following implantation of nitrogen at room temperature and after a series of *in situ* annealing cycles. In Figure 2 b) we show spectra for co-implantation of carbon ions following nitrogen implantation while the sample was heated to 780º C during co-implantation. The spectra show the well know features, including the diamond Raman line close to the NV^0 zero-phonon line at 575 nm, the NV$^-$ line at 637 nm and the vibronic sideband form the NV$^-$ centers. Intensities of NV-center lines change due to co-implantation and annealing but spectral feature changes, e. g. line width changes of the NV$^-$ zero phonon line due to damage accumulation [14], could not be observed in these room temperature PL measurements.

3. Results and Discussion

Figure 3 shows the evolution of NV-center PL counts during *in situ* annealing and for a series of co-implantation fluences where the co-implanted species was helium. NV$^-$ and NV^0 intensities were extracted from peak intensities in spectra like the ones shown in Figure 2. The error bar shown resulted form laser stability and alignment uncertainty in repeated measurements of the same implant spots. Trends for NV$^-$ and NV^0 intensities were similar and in Figure 3 we added intensities from NV$^-$ and NV^0 lines. NV-intensities first increase for co-implantation of only 10^{11} cm^{-2} He ions, then drop and decrease significantly for a co-implantation fluence of 10^{13} cm^{-2}. Annealing recovers the PL intensity following co-implantation with 10^{13} He/cm^2 after only 10 minutes. Extended annealing to 2 h did not show further changes of the NV-PL intensity after co-

implantation with 10^{12} He/cm^2. Annealing in specific ambients can lead to etching of diamond surfaces. The constant PL intensities for a samples annealed at 780° C for 2 h following co-implantation with 10^{12} He/cm^2 indicates that no surface etching took place in these experiments. Surface etching would reduce PL intensities especially for the relatively shallow nitrogen implants used in this study. On the other hand, we did not perform control experiments with e. g. step edge or repeated depth profiling measurements to exclude any surface etching. If there was surface etching, then the loss of material and NV-centers would have to be compensated with increasing NV-conversion during extended annealing to account for the observed constant PL intensities, which seems unlikely. The constant PL-intensity during a 2 h anneal also indicates that diffusion of NV-centers is minimal at 780° C in vacuum.

Figure 4 shows the evolution of NV-PL intensities now for co-implantation of carbon ions where the diamond sample was heated to a temperature of 780° C during co-implantation. Co-implantation increases the NV PL signal indicating that additional vacancies are captured by substitutional nitrogen atoms to form stable NV-centers. For the NV-count to increase, already formed NV's must be stable during co-implantation and annealing. We note that PL is only sensitive to NV$^-$ and NV^0 charge states of NV-centers. Tracking these, we find trends for both PL visible NV charge states to be similar. The co-implantation species and the substrate temperature affect optimal fluences for enhanced NV-formation. Above a critical fluence, further co-implantation decreases the NV-intensities. At first glance this is to be expected for diamond from many years of futile attempts to achieve reliable n-type doping. Lattice damage accumulates and solid phase epitaxial re-growth, which is so routinely used for silicon, does not occur in diamond under readily achievable laboratory conditions of temperature and pressure [12, 15]. We find that co-implantation of 10^{12} cm^{-2} carbon ions into hot diamonds enhances NV-PL intensities by about 25%.

The histogram in Figure 5 summarizes results for co-implantation of hydrogen, helium and carbon ions as a function of fluence and for samples at room temperature or heated to 780º C during co-implantation. Results are normalized to the nitrogen only implants. Annealing following co-implantation only, without prior nitrogen implantation, led only to a negligible NV-PL signal due to the low nitrogen concentrations in the substrates (Fig. 2 b).   The absolute conversion efficiencies were not measured in this studies. From previous studies we estimate these to be of order 5% [5, 7]. Further optimization of the setup will allow also PL measurements at low temperature, where relative emission intensities in the NV^0 and NV$^-$ zero-phonon lines is much enhanced. Also, counting of single center in a high resolution optical microscope will enable absolute calibration of implanted N to PL active NV-center conversion efficiencies.

The damage threshold for graphitization of diamond during annealing above a temperature of 600° C is about 10^{22} vacancies/cm^3 [12, 14, 15]. We observe a drop in the NV-PL intensity for co-implantation of 10^{13} ions/cm^2, consistently for H, He and C ions. For C-ions, ranges are about the same as for N-ions at the same implant energy and channeling does not play a significant role at the relatively low implant energy of 7.7 keV [7]. With SRIM we can estimate that each carbon ion forms about 56 vacancies in the diamond sample (assuming a density of 3.5 cm^{-3} and a displacement energy of 35 eV). The resulting damage density is only about 4×10^{20} vacancies/cm^3, a factor of 25 below the damage threshold for graphitization. Also, dynamic annealing [12, 15] at the low

dose rates used here (co-implantations were performed with beam intensities <10 nA/mm^2) can be expected to prevent damage accumulation altogether. For He and H co-implantations, we find similar trends as for C in the fluence dependence of NV-PL intensities. The damage levels and profiles for these lighter ions are, however, very different then for C. SRIM can not predict the damage profiles for H and He co-implantations under channeling conditions very well. Yet it is clear from SRIM simulations even without consideration of channeling effects that damage levels, i. e. the number of vacancies created at the shallow positions of the implanted nitrogen ions are much reduced vs. C-co-implants. For C, the vacancy density at the peak of the nitrogen depth profile of 11.5 nm is 3 vacancies / ion / nm, for He it is ten times lower and for H it is only 0.02 vacancies/ion/nm. Both the total number and the densities of vacancies are much lower for H and He vs. C-ions. This finding points towards another mechanism that leads to reduced NV-PL intensities, other then damage accumulation in the diamond lattice. The observed similar fluence dependences of NV-PL intensities for H, He and C co-implants with their very different energy loss profiles [17] indicates that target ionization and the accumulation of charged defects in the diamond lattice leads to ionization of NV-centers and is responsible for the drop of NV-PL intensities for co-implantation fluences above 10^{12} cm^2 for H, He and C ions. For C-ions, the drop is greatest, consistent with the combined effects of localized ionization and lattice damage. For H and He co-implants, the much lower lattice damage levels for co-implantation under channeling conditions are offset by ionization effects which convert NV-centers to dark states, e. g. NV$^+$, leading to the observed drop in NV-PL intensities. There is also a possibility that chemical effects could play a role for H [18] and He implants. However, the ranges of these lighter ions is much greater (60 nm for H, 40 nm for He) then that of the implanted nitrogen (peak range of 11.5 nm) at the same implant energy of 7.7 keV used for all ion species and so this seems very unlikely.

We speculate that further optimization of NV-formation will be possible when we evaluate a broader range of implantation temperatures, ion implant energies, charge compensation and annealing conditions.

4. Conclusion

We study NV-formation in single crystal CVD diamonds in an *in situ* processing chamber as a function of co-implantation and annealing conditions. Co-implantation adds vacancies, which can be captured by substitutional nitrogen atoms to form NV-centers and NV center formation is enhanced up to a critical co-implantation fluence. Co-implantation into hot substrates under conditions of dynamic annealing aids NV-formation. We discuss effects of damage accumulation and accumulation of charges in the diamond lattice due to electronic energy loss of ions during co-implantation as mechanisms responsible for decreasing NV-PL intensities for co-implantation fluences above 10^{12} cm^{-2}. Further optimization of processing conditions promises to enable NV-center formation with enhanced reliability.

Department of Energy Contract No. DE-AC02-05CH11231 and through the DARPA Quest program.

References

[1] G. D. Fuchs, V. V. Dobrovitski, D. M. Toyli, F. J. Heremans, D. D. Awschalom, Science 326, 1520 (2009)

[2] P. Neumann, et al., 6, 249 (2010); E. Togan et al., Nature 466, 730 (2010), G. De Lange et al., Science 330, 60 (2010) ; C.A. Ryan et al., Phys. Rev. Lett. 105, 200402 (2010)

[3] G. Balasubramanian, et al., Nat. Mat. 8, 383 (2009); J. M. Taylor, et al., Nature Physics 4, 810 (2008); C. L. Degen, Appl. Phys. Lett. 92, 243111 (2008)

[4] C. D. Weis, et al., J. Vac. Sci. Tech. B 26, 2596 (2008)

[5] S. Pezzagna, B. Naydenov, F. Jelezko, J. Wrachtrup, J. Meijer, New J. Phys. 12, 065017 (2010); J. Meijer, et al., Appl. Phys. Lett. 87, 261909 (2005)

[6] B. Naydenov , V. Richter , J. Beck , M. Steiner , P. Neumann , G. Balasubramanian , J. Achard , F. Jelezko , J. Wrachtrup , R. Kalish , Appl. Phys. Lett. 96, 163108 (2010)

[7] D. M. Toyli, C. D. Weis, G. D. Fuchs, T. Schenkel, D. D. Awschalom, NanoLett. 10, 3168 (2010)

[8] K. M. C. Fu, C. Santori, P. E. Barclay, R. G. Beausoleil, Appl. Phys. Lett. 96, 121907 (2010)

[9] M.V. Hauf, B. Grotz, B. Naydenov, M. Dankerl, S. Pezzagna, J. Meijer, F. Jelezko, J. Wrachtrup, M. Stutzmann, F. Reinhard, J.A. Garrido, arXiv:1011.5109v1

[10] R. Hanson, V. V. Dobrovitski, A. E. Feiguin, O. Gywat, D. D. Awschalom, Science 320, 5874 (2008)

[11] J. R. Rabeau, P. Reichart , G. Tamanyan , D. N. Jamieson, S. Prawer , F. Jelezko , T. Gaebel , I. Popa , M. Domhan , J. Wrachtrup, Appl. Phys. Lett. 88, 023113 (2006)

[12] R. Kalish, C. Uzan-Saguy, B. Phiiosoph , V. Richter, J. P. Lagrange, E. Gheeraert, A. Deneuville, A.T. Collins, Diamond and Related Materials 6, 516 (1997)

[13] S. Pezzagna, et al., Small, 6, 2117 (2010)

[14] F. C. Walderman, et al., Diamond & Related Materials 16, 1887 (2007)

[15] R. Kalish and S. Prawer, Nucl. Instr. Meth. B 106, 492 (1995)

[16] A. T. Collins, J. Phys. Cond. Matt. 14, 3743 (2002)

[17] SRIM, The Stopping and Ranges of Ions in Matter, J. Ziegler, www.SRIM.org

[18] C. Glover, M. E. Newton, P. Martineau, D. J. Twitchen, J. M. Baker, Phys. Rev. Lett. 90, 185507 (2003)
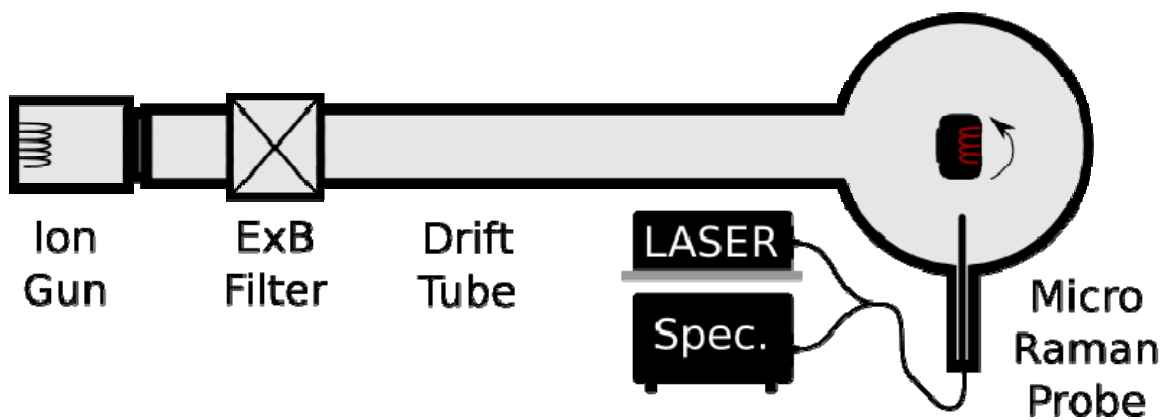
Figure 1. Schematic of the experimental setup with ion source, mass analyzer (ExB filter), vacuum chamber, goniometer with heatable sample holder and fiber coupled excitation laser and spectrometer.
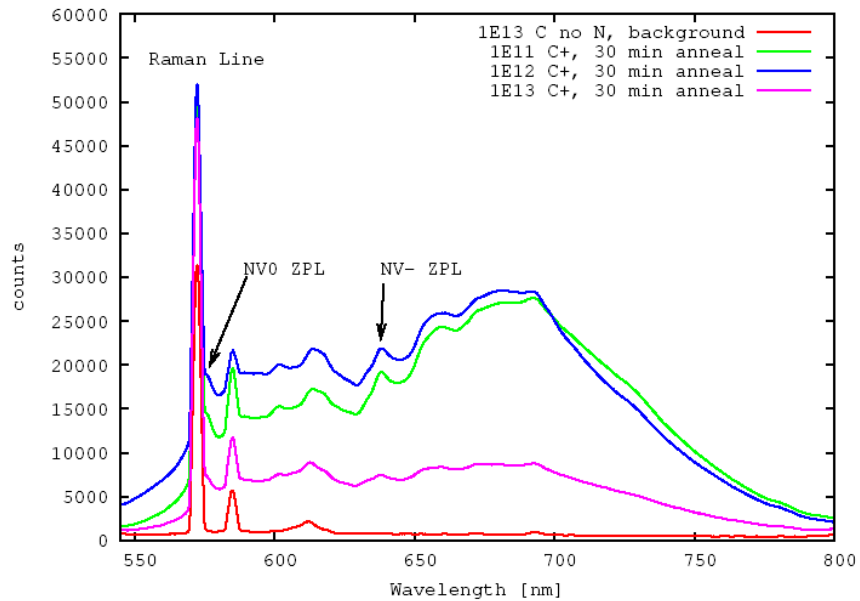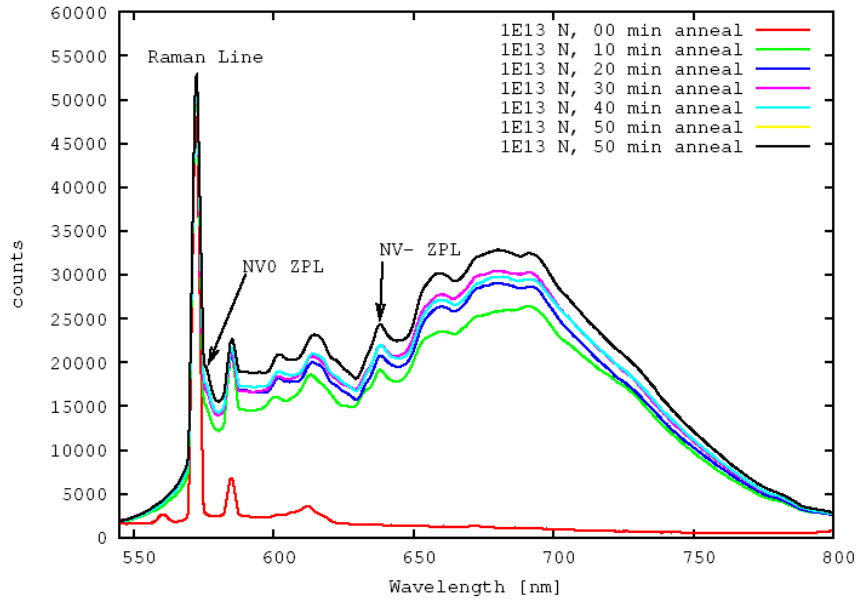
Figure 2: Examples of PL spectra (room temperature) from diamond samples following implantation of a) nitrogen ions (10^{13} cm^{-2}) and for a series of annealing times, b) for N-implantation followed by co-implantation of carbon ions with the sample at 780ºC during implantation (10^{11}, 10^{12} and 10^{13} cm^{-2}). The red curve in b) shows the background spectrum from a diamond sample that was implanted with C only, without prior N-implantation.
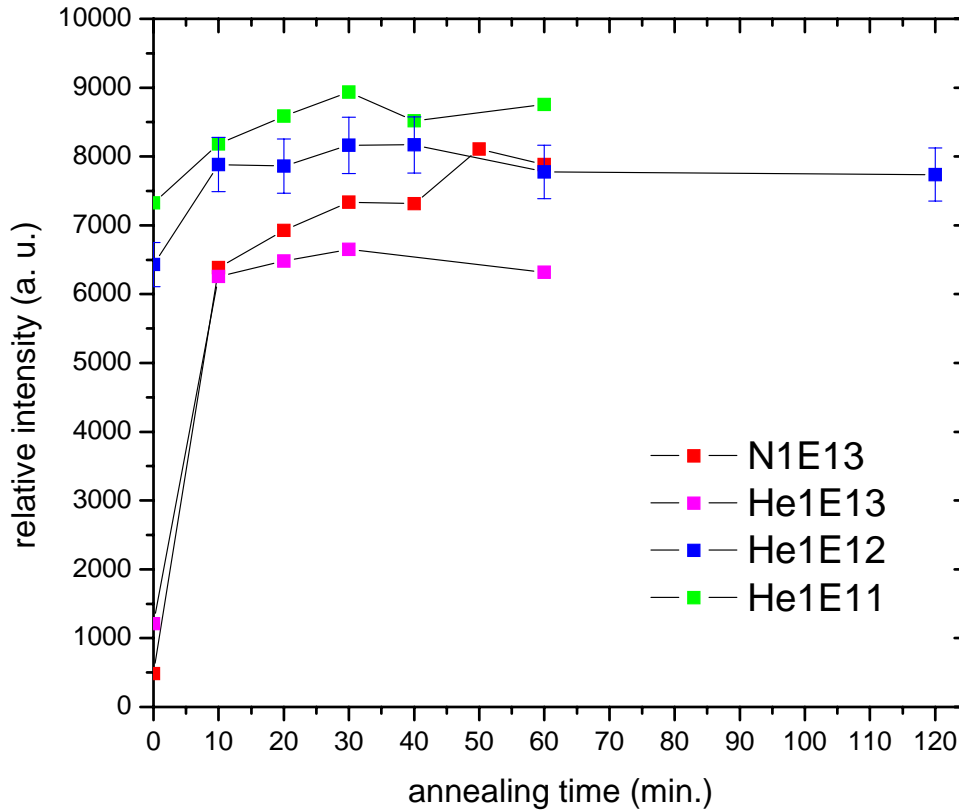
Figure 3: PL intensities from NV-centers (NV$^-$ plus NV^0) as a function of annealing time and for a series of co-implantation fluences for co-implantation with helium ions (7.7 keV, normal incidence) at room temperature. Note that co-implantation with 10^{13} cm^{-2} He$^+$ ions decreases the NV-count significantly but annealing for only 10 minutes recovers most of the NV's. Representative error bars are shown for the 10^{12} cm^{-2} co-implant series. Lines are drawn to guide the eye.
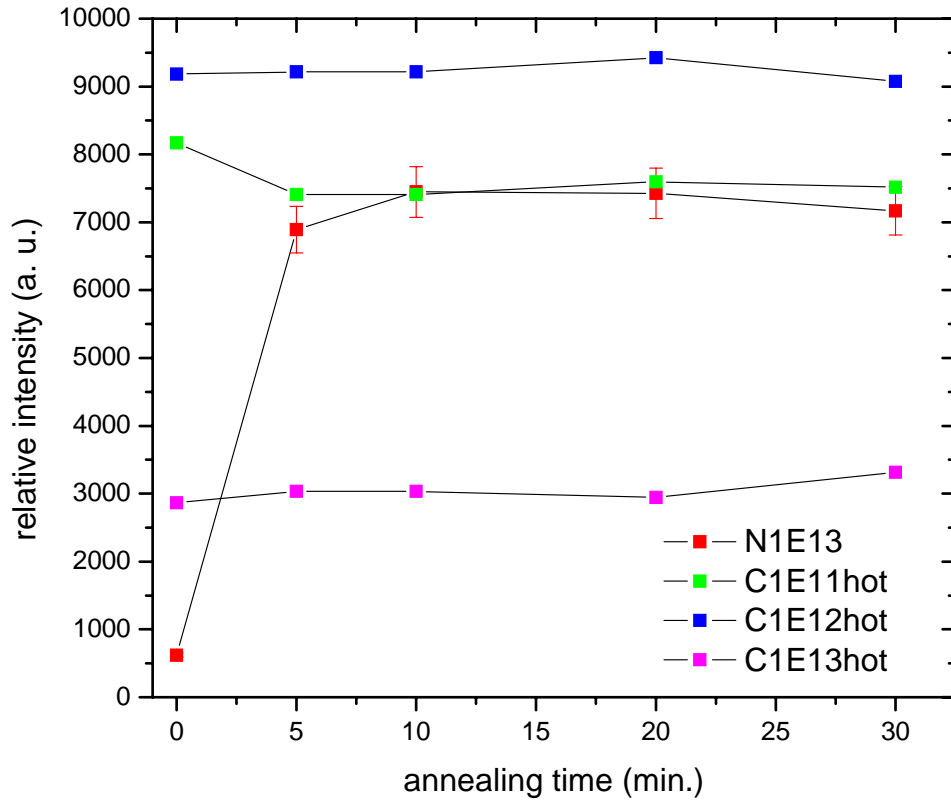
Figure 4: PL intensities from NV-centers (NV$^-$ and NV^0) as a function of annealing time and for a series of co-implantation fluences for co-implantation with carbon ions (7.7 keV, normal incidence) and with diamonds heated to 780° C during co-implantation. Representative error bars are shown for the N-only implant series (10^{13} cm^{-2}, 7.7 keV, normal incidence). Lines are drawn to guide the eye.
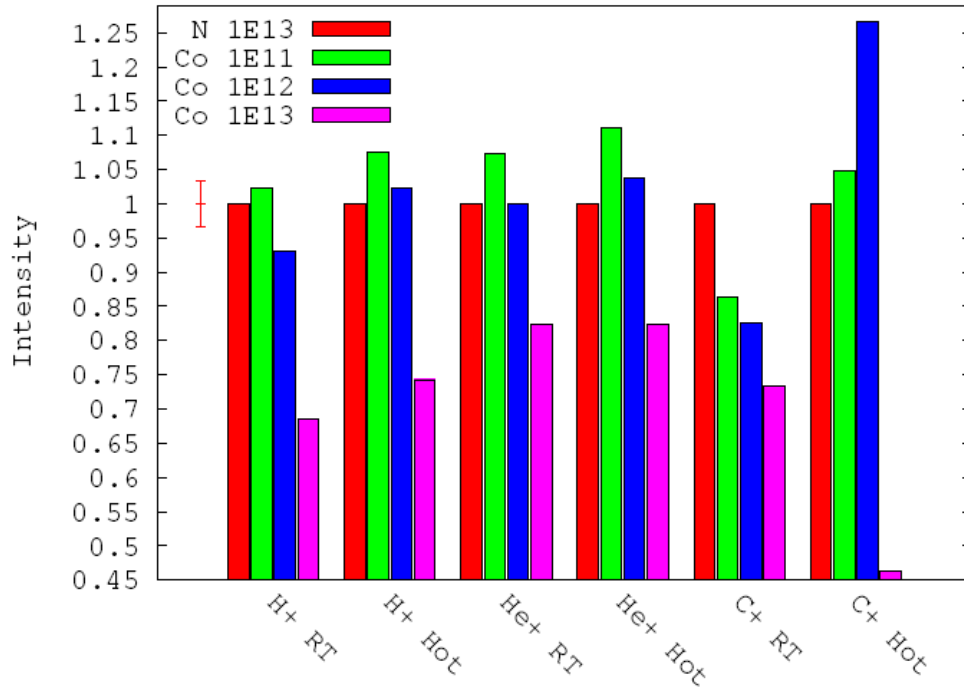
Figure 5: Histogram summarizing the NV-PL intensity evolution for co-implantation of hydrogen, helium and carbon ions (all 7.7 keV, normal incidence) into diamond samples held at room temperature or heated to 780°C during implantation. A representative error bar is shown for the N-only implant in the Hydrogen co-implantation at room temperature series.

DISCLAIMER